View metadata, citation and similar papers at core.ac.uk

brought to you by CORE

provided by Elsevier - Publisher Connector

Biochimica et Biophysica Acta 1828 (2013) 2121–2133

Contents lists available at SciVerse ScienceDirect

Biochimica et Biophysica Acta

journal homepage: www.elsevier.com/locate/bbamem

Progressive stages of mitochondrial destruction caused by cell toxic bile salts

Sabine Schulz [a], Sabine Schmitt [a], Ralf Wimmer [b], Michaela Aichler [c], Sabine Eisenhofer [d], Josef Lichtmannegger [a], Carola Eberhagen [a], Renate Artmann [b], Ferenc Tookos [d], Axel Walch [c], Daniel Krappmann [e], Catherine Brenner [f], Christian Rust [b], Hans Zischka [a,*]

[a] Institute of Molecular Toxicology and Pharmacology, Helmholtz Center Munich, German Research Center for Environmental Health, Ingolstaedter Landstrasse 1, D-85764 Neuherberg, Germany
[b] Department of Medicine 2 — Grosshadern, University of Munich, D-81377 Munich, Germany
[c] Research Unit Analytical Pathology — Institute of Pathology, Helmholtz Center Munich, German Research Center for Environmental Health, D-85764 Neuherberg, Germany
[d] Institute of Biomathematics and Biometry, Helmholtz Center Munich, German Research Center for Environmental Health, D-85764 Neuherberg, Germany
[e] Research Unit Cellular Signal Integration, Institute of Molecular Toxicology and Pharmacology, Helmholtz Center Munich, German Research Center for Environmental Health, Ingolstaedter Landstraße 1, D-85764 Neuherberg, Germany
[f] INSERM UMR-S 769, LabEx LERMIT, Châtenay-Malabry, F-92296, France

ARTICLE INFO

Article history:
Received 8 February 2013
Received in revised form 26 April 2013
Accepted 7 May 2013
Available online 17 May 2013

Keywords:
Mitochondria
Bile salts
Cholestasis
Mitochondrial permeability transition
Liver

ABSTRACT

The cell-toxic bile salt glycochenodeoxycholic acid (GCDCA) and taurochenodeoxycholic acid (TCDCA) are responsible for hepatocyte demise in cholestatic liver diseases, while tauroursodeoxycholic acid (TUDCA) is regarded hepatoprotective. We demonstrate the direct mitochondrio-toxicity of bile salts which deplete the mitochondrial membrane potential and induce the mitochondrial permeability transition (MPT). The bile salt mediated mechanistic mode of destruction significantly differs from that of calcium, the prototype MPT inducer. Cell-toxic bile salts initially bind to the mitochondrial outer membrane. Subsequently, the structure of the inner boundary membrane disintegrates. And it is only thereafter that the MPT is induced. This progressive destruction occurs in a dose- and time-dependent way. We demonstrate that GCDCA and TCDCA, but not TUDCA, preferentially permeabilize liposomes containing the mitochondrial membrane protein ANT, a process resembling the MPT induction in whole mitochondria. This suggests that ANT is one decisive target for toxic bile salts. To our knowledge this is the first report unraveling the consecutive steps leading to mitochondrial destruction by cell-toxic bile salts.

© 2013 Elsevier B.V. All rights reserved.

1. Introduction

Mitochondria are critically involved in the induction of cell death. A decisive event is the induction of the mitochondrial permeability transition (MPT), an unspecific increase of the inner mitochondrial membrane permeability up to 1.5 kDa. Upon MPT induction, a colloid-osmotically driven influx of water into the mitochondrial matrix ("swelling") occurs, causing mitochondrial structure changes [1], and culminating in the distension and rupture of the outer membrane (MOMP) [2–4]. MOMP liberates Cyt C into the cytosol, the hallmark signal towards cell death [5–7]. In cell free systems, the MPT is typically assessed by an optical density (OD) decrease in mitochondrial suspensions due to mitochondrial swelling, a direct consequence of MPT induction.

Mechanistically the MPT is still a conundrum. Two major mechanistic MPT models, termed "classical" and "alternative" have been suggested. The classical model claims a non-selective pore formed by proteins from either the inner or both mitochondrial membranes [8,9]. However, the molecular constituents of the MPT pore are still under debate [5,6,9–11]. In contrast, the alternative model proposes denaturations/rearrangements of membrane proteins to cause MPT [12]. At present, it is also unclear whether the MPT, elicited by diverse stimuli, is mechanistically a uniform process resulting in equally damaged mitochondria or whether different stages of damage result from these stimuli. This question is of particular importance with respect to the ongoing discussion about the implication of the MPT in different cell death scenarios like apoptosis or necrosis [5–7,13–17].

Abbreviations: ANT, adenine nucleotide translocator; Cyt C, cytochrome C; Cys A, cyclosporine A; FCCP, carbonylcyanide-p-(trifluoromethoxy) phenyl-hydrazone; GCDCA, glycochenodeoxycholic acid; IM, inner membrane; MβCD, methyl-β-cyclodextrin; MMP, mitochondrial membrane potential; MOMP, mitochondrial outer membrane rupture; MPT, mitochondrial permeability transition; 4-MUP, 4-methylumbelliferyl phosphate; OD, optical density; OM, outer membrane; PC, phosphatidylcholine; Rh123, rhodamine 123; ROS, reactive oxygen species; TCDCA, taurochenodeoxycholic acid; TUDCA, tauroursodeoxycholic acid; VDAC, voltage-dependent anion channel; ZE-FFE, zone electrophoresis in a free flow electrophoresis device

* Corresponding author. Tel.: +49 89 3187 2663; fax: +49 89 3187 3449.
E-mail address: zischka@helmholtz-muenchen.de (H. Zischka).

0005-2736/$ – see front matter © 2013 Elsevier B.V. All rights reserved.
http://dx.doi.org/10.1016/j.bbamem.2013.05.007

Glycine- and taurine-chenodeoxycholate (GCDCA and TCDCA) are the predominant hydrophobic bile salts accumulating in cholestatic patients, and account for liver cell death [18–22]. Bile salt-dependent mitochondrio-toxicity has been firmly established by several studies [23], which have demonstrated that bile salts impair the inner mitochondrial transmembrane potential (MMP) [24] and induce the MPT [24–26]. It remained, however, unclear how this mitochondrial destruction proceeds in detail, as such deleterious effects were especially detected in the presence of markedly elevated calcium (e.g. 50 μM in [24]), or with highly toxic doses of GCDCA [25,26].

In this report, we compared the mitochondrio-toxicity of GCDCA, TCDCA, TUDCA and the "classical" MPT-inducer calcium. OD measurements of mitochondrial suspensions demonstrate the MPT induction upon cell toxic bile salt exposure. However, we find that this approach is of limited use in order to reveal the detailed sequence of mitochondrial destruction elicited by GCDCA and TCDCA. We therefore concentrate on an alternative approach, using zone electrophoresis in a free-flow device (ZE-FFE), in order to separate mitochondria with progressive membrane damages, i.e., losses of outer membrane parts, upon bile salt exposure [27,28]. We find that bile salts initially bind to the mitochondrial outer membrane and mediate structural alterations of the inner boundary membrane, i.e., the inner membrane parts directly adjacent to the outer membrane. Subsequently, a significant increase of the inner membrane permeability irreversibly directs the mitochondria towards MPT and MOMP. As these findings point to a destructive progression of the bile salts via the mitochondrial membranes, we further concentrated on the participation of two major abundant mitochondrial proteins residing in the outer and inner mitochondrial membrane, VDAC and ANT respectively. To that end we employed dye-loaded liposomes reconstituted with these proteins, which especially point to the inner membrane protein ANT to mediate the process of toxic bile salt derived mitochondrial destruction. To our knowledge, this is the first report, which dissects the mitochondrial destruction into defined stages upon direct exposure to cell-toxic bile salts in the patho-physiological concentration range. This study may therefore serve as a blueprint for the elucidation of mitochondrio-toxic events elicited by other pathological situations or chemical exposures.

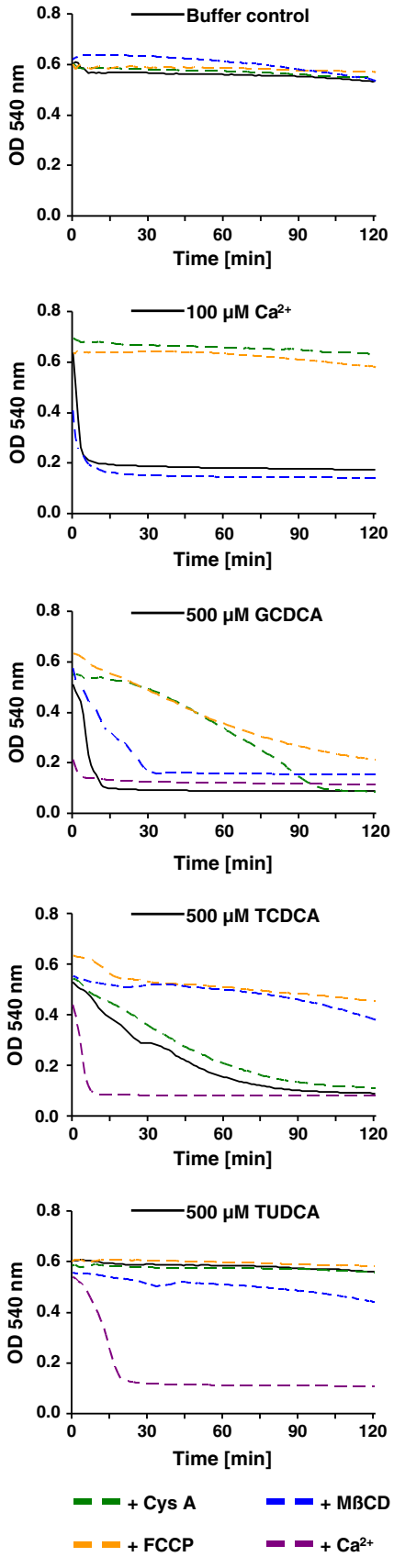

2. Material and methods

2.1. Mitochondrial analyses

Fresh rat liver mitochondria were essentially isolated as described elsewhere [29]. In brief, cell debris of homogenized rat liver tissue was removed by two consecutive centrifugations (800 × *g*, 10 min each). Thereafter, mitochondria were pelleted from the supernatant (9000 × *g*, 10 min), further purified by Percoll™ density gradient centrifugation (9000 × *g*, 10 min), subsequently washed and finally pelleted at 9000 × *g* [29]. Isolated mitochondria were subjected to quantification and kept on ice until use. Membrane potential (MMP) was monitored by the rhodamine 123 quenching method at Ex 485/20 nm, Em 528/20 nm [30] in 96-well plates containing 3 mg/ml freshly isolated mitochondria in a Synergy2 plate reader (BioTek, Bad Friedrichshall, Germany). FCCP (1 μM) served as internal control for MMP dissipation. MPT-induction was followed by light scattering at 540 nm in 1 min intervals for 2 h under the same conditions as for MMP. Parallel monitoring of MMP–MPT (Fig. 2) was done as above in the same wells. Measuring intervals were 1 min 13 s with 31 s delays for MPT and MMP measurements. In control experiments independence of both assessed parameters was validated. Results were directly exported into Excel to display the respective MMP/MPT curves (Fig. 1, S1, 2A–C upper panels, S2A–E upper panels).

Fig. 1. Pharmacological interventions demonstrate the mechanistic difference of calcium and bile salt mediated MPT. Optical density measurements ($OD_{540\ nm}$) of freshly isolated rat liver mitochondria incubated with buffer (control), 100 μM calcium or 500 μM bile salts (control: n = 7, Ca^{2+}: n = 6, GCDCA: n = 5, TCDCA: n = 3, TUDCA: n = 4) and co-incubated with either 5 μM Cys A (control: n = 3, Ca^{2+}: n = 6, GCDCA: n = 5, TCDCA: n = 3, TUDCA: n = 4), or 1 μM FCCP (control: n = 9, Ca^{2+}: n = 7, GCDCA: n = 9, TCDCA: n = 6, TUDCA: n = 2), or 500 μM MβCD (n = 4), or upon a mitochondrial calcium preload (20 μM; GCDCA: n = 5, TCDCA and TUDCA: n = 3).

2.2. Zone electrophoresis in a free-flow device

Zone electrophoresis in a free flow electrophoresis device (ZE-FFE) is an adequate tool for the purification and preparative analysis of mitochondria isolated from various sources, such as yeast, plants or liver tissues [31–34]. In ZE-FFE, charged particles are injected into a laminar buffer stream, deflected by a perpendicular oriented electrical field, and collected at the end of the separation chamber [27]. As the mitochondrial inner membrane from rat liver mitochondria differs in surface charge from the enveloping outer membrane [27,28,35], ZE-FFE can detect whether mitochondria have undergone an MPT-induced MOMP, due to the resulting exposure of more negative inner membrane charges [27,28]. The more the outer membrane is stripped off by MPT from the mitochondria, the more the resulting remnants shift towards the anode [27,28]. Here we used this approach to separate bile salt treated mitochondria that have undergone actual MPT with MOMP, from mitochondria with an intact outer membrane.

Freshly isolated rat liver mitochondria were challenged with 500 μM GCDCA, TCDCA, or TUDCA as indicated in Figs. 3, S3 and 4. Reference ZE-FFE profiles were buffer or calcium (100 μM) treated mitochondria; 10 min incubation time each. Subsequently mitochondria were pelleted, resuspended in separation buffer and subjected to ZE-FFE at the cathodal side with a sample flow rate of 1–2 ml/h. Electrophoresis was performed at 750 V in horizontal mode at 4 °C as described in detail elsewhere [27,31,34,36]. Mitochondrial populations were collected in 96-well plates and separation was followed at 260 nm in a plate reader (μQuant, BioTek, Bad Friedrichshall, Germany) [36]. Results were directly exported into Excel to display the separation profiles, wherein fraction 1 is most anodal and fraction 96 cathodal. For the sake of clarity, the deflection ranges of the mitochondrial populations are displayed (fraction 40 to 60). Peak fractions were collected for further analysis.

2.3. ANT-isolation from rat hearts

ANT was isolated essentially as described [37] using mitochondria purified by differential centrifugation from four rat hearts each. Mitochondria were solubilised with 6% Triton X-100 and supernatants loaded on hydroxyapatite columns (BioRad, Munich, Germany), eluted and diluted with low concentration (0.5%) Triton X-100 buffer and further purified by a "HiTrapSP" cation exchanger column (GE Healthcare, Munich, Germany), linked to a FPLC system. ANT was eluted by a 0–1 M NaCl gradient and FPLC fractions were analyzed for ANT content by immunoblot analysis and checked for purity/cross-contamination with VDAC.

2.4. VDAC-isolation from rat liver

VDAC was isolated according to de Pinto et al. [38]. Rat liver mitochondria were solubilised with 3% Triton X-100 followed by a 1 h ultracentrifugation at 100,000 ×*g*. Supernatants were purified by a hydroxyapatite:celite®535 column (2:1) (BioRad, Munich, and Roth, Karlsruhe, Germany). VDAC was eluted with 0.5% Triton X-100, pH 7.0. Eluate fractions were checked for VDAC content and ANT cross-contamination by immunoblot analysis.

2.5. ANT and VDAC reconstitution in liposomes and test assay

Liposome preparation and protein reconstitution into liposomes were done as described [39]. As phosphatidylcholine, phosphatidylethanolamine and phosphatidylinositol are major phospholipid species in rat liver mitochondrial membranes [40,41] we used a soybean extract (Sigma, Munich, Germany), enriched in L-α-phosphatidylcholine (14–23%) but also containing phosphatidylethanolamine and phosphatidylinositol in order to roughly mimic these mitochondrial membrane constituents. While this composition neglects the specific presence of cholesterol and cardiolipin in the mitochondrial outer and inner membranes, respectively, we have chosen this identical phospholipid composition for the reconstituted proteoliposomes in order to limit the experimental differences to the embedded membrane proteins. The approximated fatty acid composition includes 20% palmitic, 5% stearic, 10% oleic, 59% linoleic and 7% linolenic acids (Sigma, Munich, Germany). The soybean extract was dissolved in chloroform, nitrogen dried and resuspended under agitation. 3 ml of solution was incubated for 20 min with either 3 ml of 125 mM sucrose, 10 mM HEPES, pH 7.4 (liposomes), 3 ml of ANT or 3 ml of VDAC (ANT- or VDAC-proteoliposomes), respectively. Liposomes and proteoliposomes were dialysed over night, aliquoted and either stored at −80 °C or immediately tested for their sensitivities towards bile salts. Thereto 4-methylumbelliferyl phosphate (4-MUP) was entrapped in liposomes and proteoliposomes by sonification upon residual dye removal by a Sephadex G25 column (GE Healthcare, Munich, Germany). Sensitivity against 1 to 2 h challenges of GCDCA, TCDCA, or TUDCA was assessed by dye release from the liposomes/proteoliposomes, detected after enzymatic conversion using alkaline phosphatase (Roche, Mannheim, Germany) by fluorescence (Ex: 360/40 nm, Em: 460/40 nm) in a Synergy2 plate reader (BioTek, Bad Friedrichshall, Germany). Data were directly exported to Excel. Self-fluorescence of GCDCA, TCDCA, and TUDCA was subtracted from fluorescence values of liposomes/proteoliposomes. Triton X-100 was used to determine maximal dye release.

2.6. Miscellaneous

Protein quantifications were done by the Bradford assay. Immunoblotting was done according to Ref. [42]. Blots were digitalized with a GS-710 Calibrated Imaging Densitometer (BioRad, Munich, Germany). Blots (Fig. S5) and displayed sections (Figs. 3, 4 and S4) were adjusted for brightness, contrast, and black/white balance by Adobe Photoshop CS3 Extended. Electron microscopy of the mitochondrial populations was done as previously described [27] on a Zeiss EM 10 CR electron microscope with the Soft Imaging Viewer (Olympus Soft Imaging Solutions GmbH, Münster, Germany). Micrographs were adjusted for brightness, contrast, and black/white balance by Adobe Photoshop CS3 Extended. Detection of mitochondrial bound bile salts by gas chromatography was done as previously described [43].

2.7. Statistics

Statistics were performed in Excel using *t*-test. Data were tested unpaired and two-tailed. Differences were denoted statistically significant with $^{*} = p < 0.05$, $^{**} = p < 0.01$, $^{***} = p < 0.001$.

3. Calculation

3.1. Parameter definition for quantitative MPT and MMP comparison

For the quantitative comparison of the mitochondrial responses to toxic bile salt challenge in terms of MPT- and MMP-measurements, we defined threshold parameters for MPT and MMP-loss start and finish time points. We calculated the slopes of MPT- and MMP-measurement curves, using the "gradient" option of the software MATLAB. For smoothing, averages of slope values were calculated for each data point using the preceding and subsequent data points. Corresponding slope profiles are displayed directly below the MMP/MPT curves (cf. Fig. 2A–C, and Fig. S2A–E). Based on the slopes of buffer treated control mitochondria, we defined the thresholds for MPT and MMP-loss start and finish. Here we determined a slope ≥1 for the beginning of MMP loss and a slope of <−0.003 for swelling/MPT start. The reverse values marked the end of these processes. Based on the start, end and slope values, we quantitatively determined the duration of the MMP-loss/MPT processes, as well as the time points when these processes become maximal (i.e. maximal slopes).

Start/end time points (triangles) and the time points of maximal slopes (boxes) were subsequently determined from the curve slopes by the "findpeaks" option in MATLAB. Results were displayed by the "plot" and "bar" options of MATLAB (cf. Figs. 2A–C lower panels, S2A–E lower panels 2D, and S2F respectively). The bar lengths depict the duration of the MPT (solid line) and MMP-loss (dashed line), respectively.

This approach offers two main advantages. First, compared to the measured curves, the slope profiles better visualize the kinetics of the MMP-loss and MPT (cf. Fig. 2A–C). Second, this curve sketching enables a quantitative analysis of the MMP/MPT in a time dependent fashion.

4. Results

4.1. Bile salt mediated direct mitochondrio-toxicity differs from calcium dependent impairment

In chronic cholestasis, hepatocytes die upon elevated levels of the toxic bile salts GCDCA and TCDCA [44], which can reach intracellular

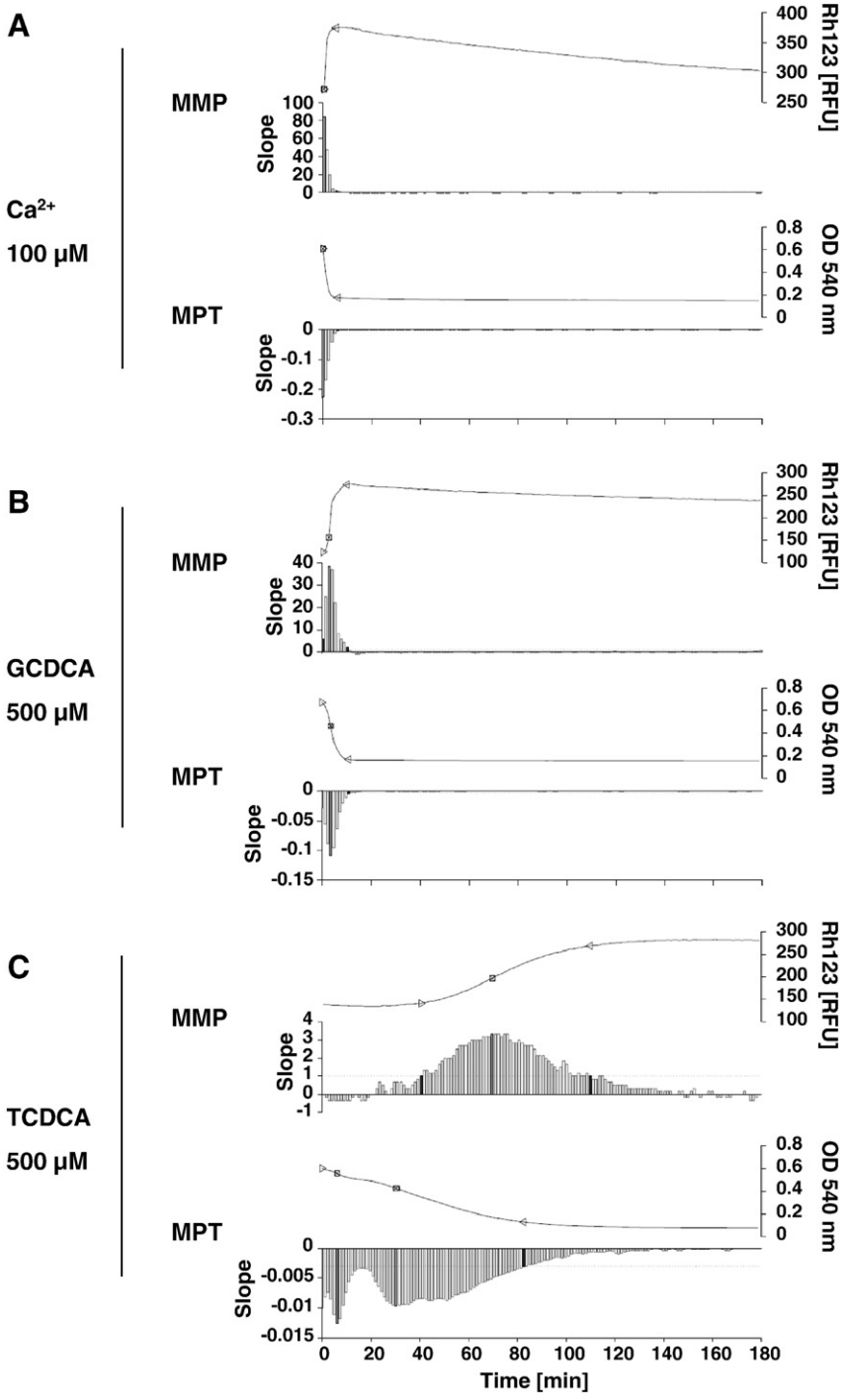

Fig. 2. Bile salts paradoxically inverse MMP-loss and MPT-induction. Simultaneous measurements of MPT induction ($OD_{540\ nm}$) and MMP loss (Rh123 fluorescence) of freshly isolated rat liver mitochondria upon bile salt challenges in comparison to calcium. A–C MMP and MPT measurement curves (upper panels) with their corresponding slopes (lower panels). Ca^{2+}: n = 7, GCDCA: n = 5, TCDCA: n = 8. D Bar charts of MMP/MPT double measurements. Bar length depicts MPT and MMP loss duration, respectively. Triangles indicate start and end points; boxes signify inflection points. Ca^{2+}: n = 7 (100 µM), GCDCA: n = 5 (500 µM), TCDCA: n = 8 (500 µM), GCDCA and TCDCA: n = 6 (250 µM), n = 5 (125 µM).

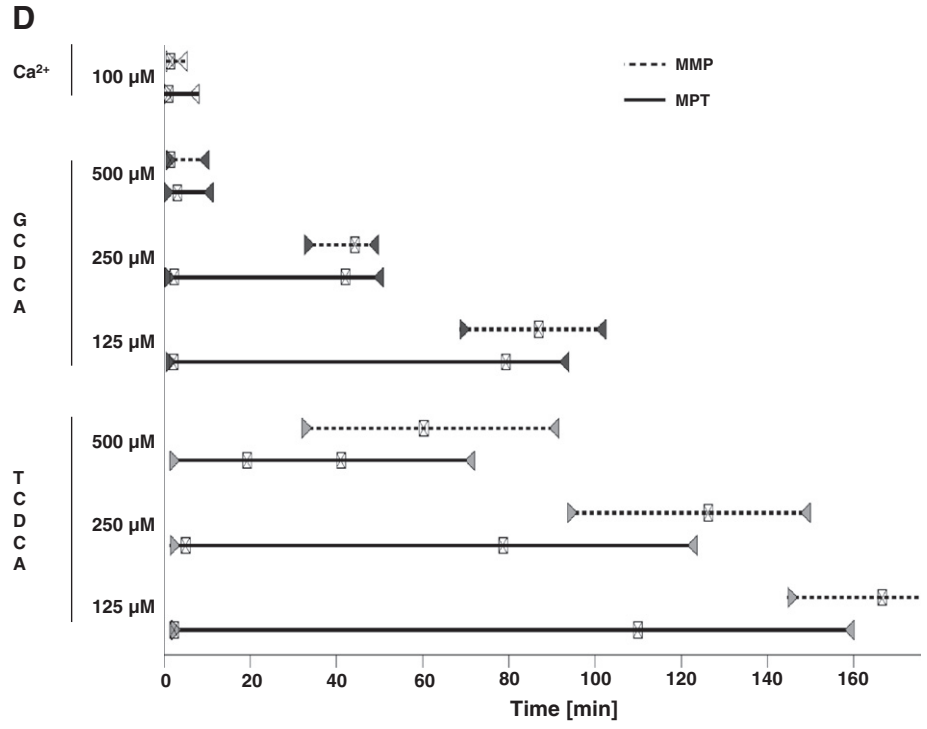

Fig. 2 (*continued*).

concentrations of up to 800 µM [45,46]. This cellular demise is largely involving mitochondria, as upon incubation, exposed hepatocytes lose their MMP [43]. Freshly isolated rat liver mitochondria undergo the MPT upon exposure to cell-toxic bile salts at pathological relevant concentrations ranging from 125 µM to 500 µM, with GCDCA being more toxic than TCDCA (Fig. 1, Fig. S1A, B). Moreover, upon co-incubation with low-dose calcium (20 µM), the GCDCA or TCDCA-induced MPT rate is drastically accelerated, pointing out to a synergistic deleterious effect of bile salts and calcium on mitochondria (Fig. 1). TUDCA does not elicit the MPT (Fig. 1). A calcium/TUDCA co-incubation is identical to the delayed MPT onset elicited by 20 µM calcium alone (Fig. 1). We therefore asked whether bile salts and calcium attack the mitochondrial membranes via the same molecular mechanism or whether their deleterious action can be distinguished experimentally. For this purpose, we tested the effects of Cys A, an inhibitor of calcium-induced MPT [47], FCCP, which destroys the MMP, thereby avoiding calcium uptake and MPT-induction, and MβCD, which is known to bind bile salts (Fig. 1).

Both Cys A and FCCP abolish calcium-induced MPT, but only decelerate GCDCA or TCDCA induced swelling (Fig. 1). On the contrary, MβCD has no influence on calcium-induced MPT, but delays GCDCA- or TCDCA-provoked MPT in a dose dependent fashion (Fig. 1, Fig. S1C, D). TUDCA does not elicit the MPT (Fig. 1). Thus, the bile salts induced MPT differs mechanistically from the calcium-elicited MPT.

4.2. Toxic bile salts paradoxically inverse MMP-depletion and MPT-onset

As FCCP instantly destroys the MMP [48], but retards the MPT onset evoked by bile salts, we further investigated the relation between MPT induction and MMP-loss.

Mitochondrial suspensions were challenged by either high dose calcium or varying doses of bile salts. MMP and MPT were simultaneously assessed from the same samples (Fig. 2). The upper panels of Fig. 2A–C display MMP (Rh123 fluorescence) and MPT ($OD_{540\ nm}$) curves. We aimed at a quantitative comparison of these mitochondrial responses in a time-dependent fashion. Therefore, we calculated the corresponding slope profiles of the MMP and MPT curves, respectively (displayed directly below the MMP/MPT curves, Fig. 2A–C, and Fig. S2A–E). This approach offers several advantages. First, compared to the measured curves, the slope profiles better visualize the kinetics of the MMP-loss and MPT (Fig. 2A–C). Second, based on the slopes of buffer treated control mitochondria, it allows defining thresholds for starting and end points of MMP-loss and MPT. Here we determined a slope ≥ 1 for the beginning of MMP loss and a slope of <-0.003 for swelling/MPT start. The reverse values marked the end of these processes. Third, based on the start, end and slope values, one can quantitatively determine the duration of the MMP-loss/MPT processes, as well as the time points when these processes become maximal (Fig. 2D). Thus, this curve sketching enables a quantitative analysis of the MMP/MPT in a time dependent fashion.

This analysis verified that calcium causes the instant and almost simultaneous onset of both swelling and MMP-loss, whereby MMP-loss finishes slightly before MPT (05:22 ± 02:49 vs. 08:10 ± 02:36 min, Fig. 2D). Thus, upon calcium challenge, the MMP-loss precedes the MPT. High dose GCDCA (500 µM) gives a similar result (Fig. 2D). TUDCA remains non-toxic in all experiments (data not shown).

TCDCA and lower concentrations of GCDCA (250/125 µM) cause an instant drop in $OD_{540\ nm}$, indicative of immediate mitochondrial swelling. Surprisingly, however, the MMP-loss is postponed in a concentration-dependent manner (Figs. 2C, D, S2A–D). Thus, under these conditions, it seems that the MPT precedes the MMP-loss.

This initial drop in $OD_{540\ nm}$ upon exposure to cell-toxic bile salt presents a clear paradox. Upon initiation of MPT, i.e., inner membrane permeabilization, a rapid passage of protons across the IM occurs, causing the MMP to instantaneously drop to zero [9]. At this point a reconsideration of the biophysical characteristics of the MPT assay merits attention. Mitochondrial suspensions are turbid and scatter light [48]. Upon MPT induction, mitochondria swell and thereby change their diffraction properties causing decreased light scattering, measured as a decline in $OD_{540\ nm}$ [48]. However, as this MPT assay basically assesses the optical density of a mitochondrial suspension in total, any (structure changing) process, that significantly affects the mitochondrial diffraction index will cause an altered OD. Thus, this assay does not only detect MPT. It therefore appears possible, that the initial OD drop upon bile salt exposure reflects mitochondrial

structure changes rather than immediate MPT-induction, since MMP is initially retained.

This hypothesis is further supported by the fact that upon TCDCA and lower concentrations of GCDCA, the elicited MPT/swelling process becomes two-phased (e.g., Fig. 2C). A fast but limited decline in $OD_{540\ nm}$ is followed by a slower but more pronounced swelling (Fig. 2C MPT curve), which is clearly apparent in the corresponding slope profile (Fig. 2C MPT slope). It is known that upon induction of the MPT the volume change for the individual mitochondrion is an "all-or-nothing event" [49], and that the $OD_{540\ nm}$ changes reflect the volume change of the fraction of mitochondria that have undergone the MPT [49]. Thus, the observed two-phased $OD_{540\ nm}$ changes could be due to two OD changing processes, of which only the later one is the MPT. The fact that there is no MMP loss concomitantly occurring with the initial $OD_{540\ nm}$ changes supports this conclusion.

Upon MMP depletion with FCCP, the swelling process induced by 500 μM GCDCA is massively prolonged but not inhibited (Fig. S2E). As with TCDCA, and in contrast to 500 μM GCDCA alone, the swelling process is two-phased (Fig. S2F). Especially, the second phase of swelling, i.e., the supposed actual MPT, indicated by the second inflection point, is strongly postponed (Fig. S2F).

It therefore appears that bile salts induce a complex pattern of molecular events in mitochondria which lead to alterations in their OD. It further appears that the "classical" swelling assay is only of limited use to characterize these events.

4.3. Bile salts alter inner-mitochondrial structures culminating in membrane damage

As the combined MMP/MPT analysis suggested that cell-toxic bile salts alter mitochondria before initiating the MPT, and as these events can only unsatisfactorily be resolved by optical density measurements, we employed an alternative methodological approach:

The outer membrane rupture/permeabilization (MOMP) is the defined endpoint of the MPT [16]. Especially in liver mitochondria, the MPT-induced MOMP results in inner membrane vesicles (IMVs or "mitoplasts") [49,50]. IMVs are highly negatively charged particles which can electrophoretically be distinguished and separated from intact mitochondria [27,28,35], i.e., from mitochondria that have not undergone MOMP. We therefore used an electrophoretic approach (zone electrophoresis in a free flow device, ZE-FFE) to separate bile salt treated mitochondria that have undergone actual MPT with MOMP (i.e., IMVs), from mitochondria with an intact outer membrane.

As previously reported [27,31], intact mitochondria incubated either in test buffer alone (control) or additionally with the non-toxic TUDCA, gather in one major peak (Fig. 3A, B). In contrast, mitochondria treated with 100 μM calcium or 500 μM GCDCA immediately undergo MPT (Figs. 1, 2), which result in IMVs that significantly deflect towards the anode (Fig. 3C, D). This anodal shift is thus associated with MOMP, as also evidenced by a marked depletion of the outer membrane protein VDAC (Fig. 3F). As expected, FCCP treated mitochondria do not shift towards the anode upon calcium challenge, fully in agreement with a blocked MPT (Fig. S3B). MβCD/Ca^{2+} treated mitochondria, however, do so (Fig. S3C), confirming that MβCD does not inhibit the Ca^{2+}-induced MPT (Fig. 1).

Unlike calcium and 500 μM GCDCA, a 10 min TCDCA challenge causes several prominent peaks (Fig. 3E). Here, the broader cathodal peak contains an additional anodal shoulder peak, indicating the emergence of distinct mitochondrial subpopulations, as confirmed by electron microscopy (Fig. 3E). The most cathodal mitochondria possess a seemingly intact outer membrane, yet exhibit significant cristae remodeling (Fig. 3E-III). This finding proves our above conclusion that mitochondrial structure alterations other than MPT-induced MOMP occur upon TCDCA treatment. TCDCA mitochondria gathering in the anodal shoulder peak demonstrate a heterogeneous picture (Fig. 3E-II); and TCDCA mitochondria from the major anodal peak have an IMV structure, and therefore, are mitochondria that have undergone MPT/MOMP (Fig. 3E-I).

Furthermore, when the MPT-onset induced by GCDCA is delayed by FCCP or MβCD (Fig. 1), mitochondria with modified structures but present outer membrane are observed (Fig. S3D-II, E-II). These organelles are collected from a major but barely shifted peak (Fig. S3D, E). Thus, although the electrophoretic characteristics of these mitochondria have barely changed, their intra-mitochondrial structure clearly has (Fig. S3D-II, E-II). Moreover, as shown in Fig. S3D-II, a structural transition can be observed even within single mitochondria. Here, parts with normal structure coexist with altered parts (Fig. S3D-II). This suggests that these alterations represent an early stage of bile salt induced mitochondrial destruction, and that the IMV structures do appear at a later stage.

4.4. Successive events of TCDCA induced mitochondrial toxicity

In order to demonstrate that the structurally altered, but MOMP-negative, mitochondria (Figs. 3E-III, S3D-II and S3E-II) do represent earlier stages of a continuous destruction process that finally leads to IMVs (Figs. 3E-I, S3D-I and S3E-I), we followed the TCDCA-dependent effects on mitochondria by a time resolved ZE-FFE approach.

In contrast to intact mitochondria (Fig. 4-I, II), a 5 min TCDCA treatment already results in two subpopulations, one major barely shifted peak and one smaller more anodal peak (Fig. 4-III, IV). The mitochondria of the barely shifted peak retained their outer membranes, yet show beginning cristae remodeling (Fig. 4-IV). This is even more pronounced in mitochondria collected from the anodal peak (Fig. 4-III). In addition, in these mitochondria, the inner boundary membrane has largely disappeared (Fig. 4-III) and the mitochondria appear larger in size, an indication of a commencing mitochondrial swelling (Fig. 4-III). As incubation time increases, the major peaks progressively deflect towards the anode, (Fig. 4, 10 to 40 min). This is paralleled by cristae remodeling, retraction of the inner boundary membrane and IMV formation (Fig. 4).

We subsequently analyzed these mitochondrial subpopulations for outer membrane integrity. Loss of Cyt C is a hallmark signal for cell death induction and VDAC depletion unequivocally demonstrates MOMP (immunoblot in Fig. 4). All anodal shifted subpopulations of TCDCA treated mitochondria demonstrate a pronounced Cyt C loss (Fig. 4 III, V, VII and VIII). In addition, a progressive VDAC depletion paralleled the extent of shift towards the anode (Fig. 4 II = IV ≤ VI < V ≤ III/VIII < VII). Interestingly, a slightly higher Cyt C loss was noted in subpopulation VI compared to the similarly deflecting subpopulation IV. However, in these both subpopulations, VDAC levels remained relatively unchanged at the level of control mitochondria. This clearly suggests that small outer membrane permeabilities occur in subpopulation VI which are sufficient for a partial Cyt C loss.

Taken together these analyses demonstrate the time-dependent progression of mitochondrial destruction by TCDCA. The electron micrographs of Fig. 4 II → IV → VI → VIII → X (right column) visualize this sequential process. Starting from intact mitochondria (II), an immediate rearrangement of the cristae near by the outer membrane occurs (IV). This progressively worsens and is associated with a disappearance of the inner boundary membrane and with a partial Cyt C release (VI). Subsequently, severe mitochondrial damages occur (VIII), and it is only then that mitochondria lose their MMP (see time axis in Fig. 2D) and actually undergo MPT. Massive matrix rearrangements take place (VIII), which are accompanied by a profound Cyt C release and MOMP (immunoblot in Fig. 4). Eventually, largely IMVs are present (X), marking the end stage of the MPT.

4.5. The mitochondrial target structures for cell toxic bile ***salts***

From the above observations, two major bile salt-induced damaging events can be distinguished. An initial structure change near the outer

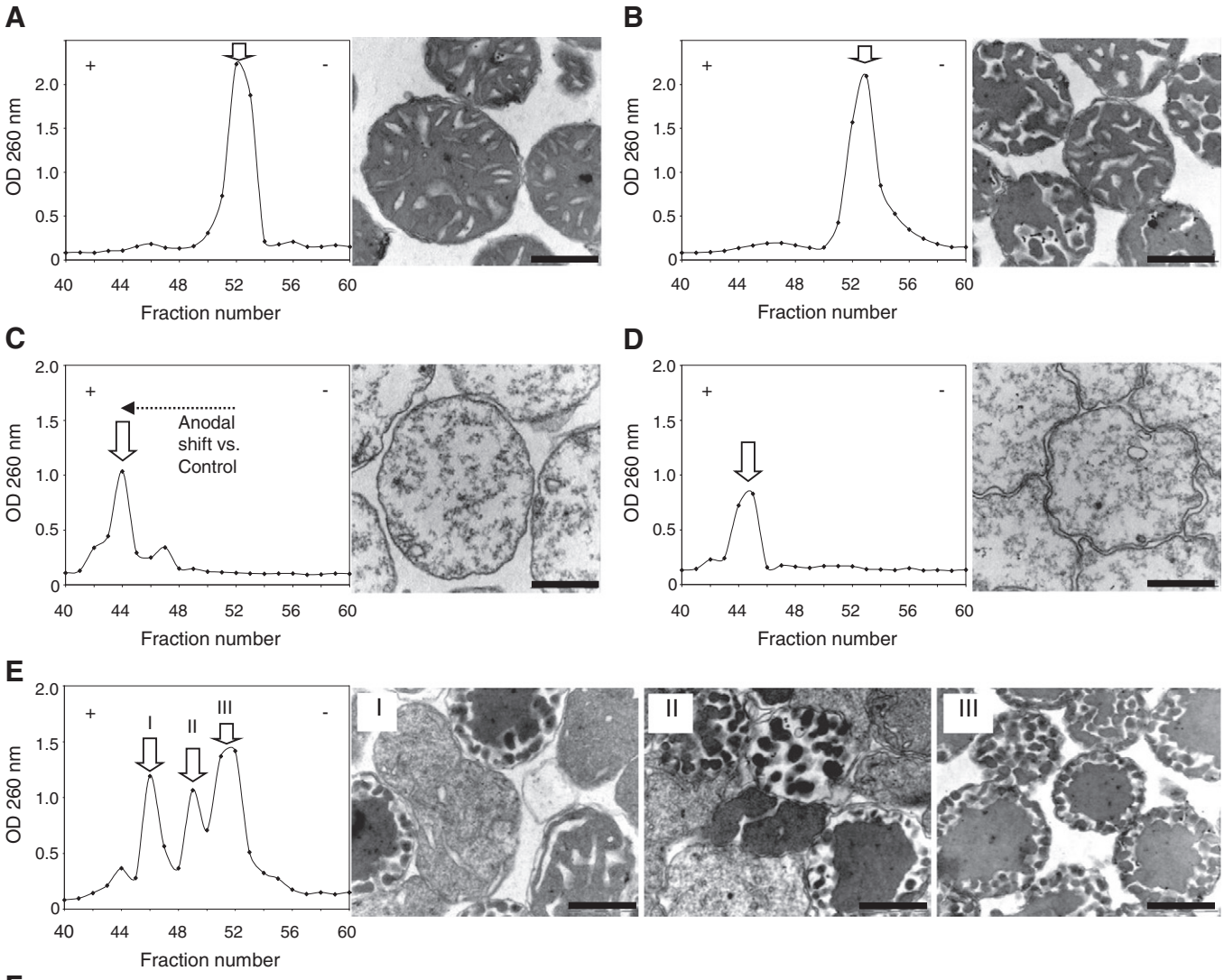

F

Control	Ca^{2+}			GCDCA					TUDCA	TCDCA		
VDAC												
ANT												
-	-	+	-	-	+	+	-	-	-	-	-	FCCP
-	-	-	+	-	-	-	+	+	-	-	-	MβCD
-	8	0	8	7	7	0	0	5	0	1	5	Anodal Shift vs. Control
3A	3C	S3B	S3C	3D	S3D-I	S3D-II	S3E-II	S3E-I	3B	3E-III	3E-I	Figure No.

Fig. 3. Bile salts cause mitochondrial structure alterations. Left panels: ZE-FFE analysis of freshly isolated rat liver mitochondria treated for 10 min with A incubation buffer (control), B 500 μM TUDCA, C 100 μM calcium, D 500 μM GCDCA or E 500 μM TCDCA bile salts. Anodal side: ⊕ cathodal side: ⊖, n = 3. Right panels: Electron micrographs of ZE-FFE partitioned mitochondria, retrieved from the indicated peaks (arrows). Bars equal 0.5 μm. F Outer membrane losses from the above separated mitochondrial populations were assessed by immunoblot analysis of VDAC with ANT as loading control.

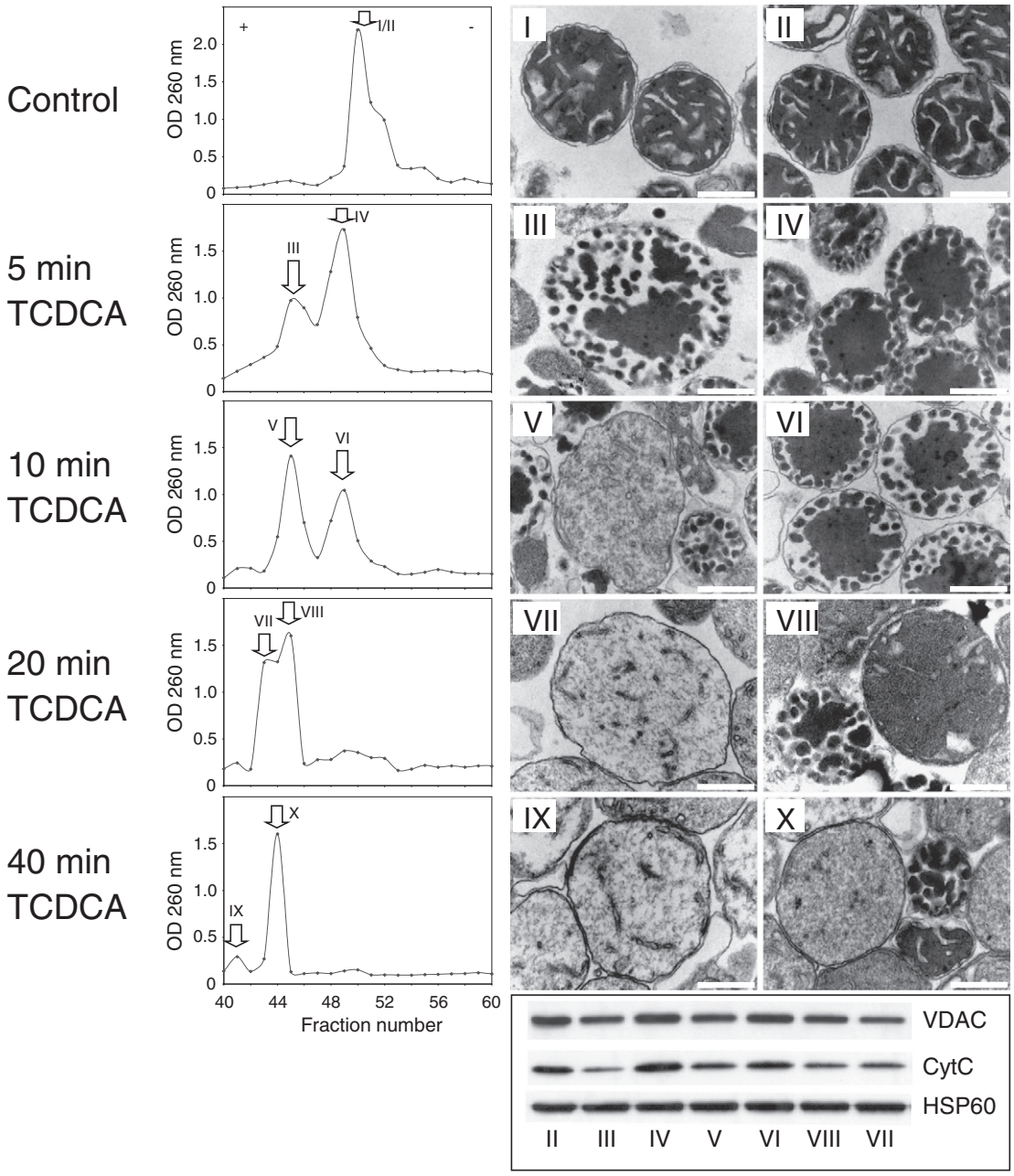

Fig. 4. Successive events of TCDCA induced mitochondrial toxicity. Left column: Time resolved ZE-FFE analysis of freshly isolated rat liver mitochondria challenged with 500 μM TCDCA. Anodal side: ⊕ cathodal side: ⊖, n = 2. Middle and right column: Electron micrographs of ZE-FFE partitioned mitochondria, retrieved from the indicated peaks (arrows). Bars equal 0.5 μm. Corresponding immunoblots reveal outer membrane losses in III, V, VII and VIII and Cyt C liberation in III, V–VIII; Hsp60 served as loading control.

membrane, characterized by cristae remodeling and disintegration of the inner boundary membrane, is followed by MMP-loss and the MPT.

As bile salts cause these profound mitochondrial membrane changes, it seems reasonable to assume that a sufficiently strong interaction between the responsible bile salts and the mitochondrial membranes occurs. We therefore asked whether the bile salts GCDCA, TCDCA, and TUDCA differ in their binding ability to mitochondrial membranes. Mitochondrial suspensions were incubated with equal doses of

Table 1
Binding of bile salts to mitochondria assessed by gas-chromatography (n = 3). In one further analysis mitochondrial bound bile salts were determined after ZE-FFE.

	GCDCA		TCDCA		TUDCA	
Bile salt bound to mitochondria	5.81 μmol/g	1.11%	11.88 μmol/g	0.87%	1.52 μmol/g	0.48%
Bile salt bound to mitochondrial subpopulations [μmol/g]	F3D 0.49		F3E-III 1.68 F3E-II 0.91 F3E-I 0.47		F3B n.d.	
Bile salt bound to mitochondrial subpopulations [%]	F3D 0.04		F3E-III 0.13 F3E-II 0.07 F3E-I 0.04		F3B n.d.	

these bile salts, subsequently washed and the amount of tightly bound bile salts was determined by gas chromatography (Table 1).

TUDCA barely binds to mitochondria, in contrast to GCDCA and TCDCA (Table 1). As TUDCA does neither induce MMP loss (not shown) nor the MPT (Figs. 1, 3B), these findings underline that a sufficiently strong mitochondrial binding of bile salts has to occur in order to elicit the deleterious events.

Interestingly, a two-fold higher amount of tightly bound TCDCA is detected when compared to GCDCA (Table 1). This finding is at first sight in contradiction with the observed higher mitochondrio-toxicity of GCDCA compared to TCDCA (Fig. 1). However, an analysis of the mitochondrial subpopulations that emerge upon bile salt exposure shows that the more the outer mitochondrial membrane is stripped of, the less bile salt can be detected in the remnant structures (Table 1). Indeed, GCDCA and TCDCA challenged mitochondria show massive outer membrane losses (Fig. 3) in the following order: $GCDCA_{anodal}$ (Fig. 3D) > $TCDCA_{anodal}$ (Fig. 3E-I) > $TCDCA_{shoulder\ peak}$ (Fig. 3E-II) > $TCDCA_{cathodal}$ (Fig. 3E-III). In this order the amounts of bound bile salts increase (Table 1), the $GCDCA_{anodal}$ (Fig. 3D) and $TCDCA_{anodal}$ (Fig. 3E-I) populations showing the lowest amount of bound bile salt. It thus appears that the reason for the detected lower amount of tightly bound GCDCA compared to TCDCA reflects the lower outer membrane content of the resulting IMVs. This, however, means that the mitochondrial outer membrane is the major target site for bile salts.

As toxic bile salts deplete the MMP and elicit the MPT, a further deleterious step subsequent to outer membrane binding must occur. This step has to disrupt the inner mitochondrial membrane integrity, which, by definition, is the unequivocal starting event for the MPT [5]. We therefore aimed at identifying the mitochondrial targets for bile salts, which are involved in the induction of the MPT. For this purpose, we employed a test system using dye-loaded (4-MUP) liposomes (Fig. 5). This molecular defined test system combines a sensitive detection system for the membrane permeabilising properties of bile salts with the possibility to specifically integrate candidate bile salt target molecules. To that end, we incorporated the isolated and purified mitochondrial inner membrane protein ANT or outer membrane protein VDAC, respectively (termed ANT/VDAC-proteoliposomes).

Non-physiologically high concentrations (2 mM) of cell toxic bile salts are required to release a significant but low amount of 4-MUP from pure liposomes (Fig. 5A Lipo). In contrast, in ANT-proteoliposomes, a slight dye release can already be detected at 250 μM TCDCA or 500 μM GCDCA, and becomes highly significant at 1000 μM (Fig. 5A, ANT). As the sensitivity towards cell-toxic bile salts is comparable between ANT-proteoliposomes and whole mitochondria (Figs. 1–4), this result suggests that the ANT protein is a target structure for cell-toxic bile salts. Moreover TUDCA, which has no effect on mitochondria, is also without effect on ANT-proteoliposomes (Fig. 5B).

Interestingly, VDAC-proteoliposomes also show a dose dependent dye release upon GCDCA or TCDCA challenge, which was, especially in the concentration range of 250–1000 μM, similar to fluorescence values obtained for ANT-proteoliposomes (Fig. 5 VDAC). This implies that integral membrane proteins have the general potential to mediate the toxicity of bile salts. It should be noted, however, that the total dye load of the VDAC-proteoliposomes almost doubled the 4-MUP content of ANT-proteoliposomes (Fig. S4A). It therefore appears that ANT proteoliposomes are more sensitive towards bile salts compared to VDAC-proteoliposomes. In addition, the higher the liposomal content of ANT is, the higher the sensitivity towards TCDCA and GCDCA (Fig. 5B). Thus, distinctive membrane proteins appear to be more sensitive towards bile salts than others and the ANT protein appears to be one crucial mediator for bile salt mitochondrio-toxicity.

5. Discussion

In this study, we demonstrate that the bile salts GCDCA and TCDCA have the toxic potential to directly destroy liver mitochondria. GCDCA and TCDCA induce the mitochondrial permeability transition (MPT) in a dose dependent fashion with GCDCA being more mitochondrio-toxic than TCDCA (Fig. 1, Fig. S1), which is in line with the established major hepatocellular toxicity of GCDCA over TCDCA in cells and whole-organ models [20,51]. In addition we confirmed the non-toxicity of TUDCA (500 μM) at the level of isolated mitochondria (Fig. 1, [52]). Moreover, in preliminary studies, we observe that co-incubation of TUDCA/GCDCA in 1:1 ratios does not prevent/delay the loss of the inner membrane potential (MMP) in liver mitochondria (data not shown). This finding agrees well with Güldütuna *et al.*, who have reported a partial, only timely restricted protective effect on mitochondria by ursodeoxycholate but not by TUDCA [52]. Although the bile salt induced MPT can be massively accelerated by calcium, it differs mechanistically from this prototype MPT inducer, as shown by differential pharmacological interventions (Fig. 1). Calcium induced MPT occurs simultaneously to the loss of the MMP (Fig. 2). In contrast, MMP-loss is delayed upon bile salt exposure (Fig. 2) but preceded by massive mitochondrial structure alterations, especially at the inner boundary membrane and the mitochondrial cristae (Fig. 3). We have uncovered these consecutive stages of mitochondrial destruction by bile salts (Fig. 4). In the final phase, MMP loss and MPT are induced, as a consequence of the bile salt attack on integral membrane proteins (Fig. 5) with the ANT as a critical target (Fig. 5).

5.1. The relevance of bile salt induced mitochondrial destruction in cholestasis

How do these findings relate to pathological in vivo situations? Typically, physiological concentrations of bile salts in hepatocytes are low (around 1–2 μM, [53]). In cholestasis, however, a tremendous intra-hepatocyte increase in GCDCA and TCDCA concentrations occurs. Under these conditions, intracellular bile salt concentrations reaching 800 μM have been reported [45,46], and 8–10% of the intracellular accumulating bile salts "tightly bind" to mitochondria [54,55].

Due to the planar/disk shaped structure of bile salts, there is a general consensus that these molecules lie flat at membrane interfaces and, in contrast to e.g., phospholipids or cholesterol, not perpendicular to the interface (e.g., [56,57]). However, resulting from molecular interactions, e.g. with polar head groups of phospholipids, their orientation within the membrane may subsequently change ([57], and references therein, [58]). A prerequisite for both, the sustained presence as well as the orientation alterations of bile salts, is their sufficiently strong binding to and/or interaction with the membrane, which is governed by the hydrophobic face of the bile salt steroid structure, ionic interactions and hydrogen bonding (see below, [57]). Here, we therefore use the term "tightly bind" to emphasize this sustained presence, which resists subsequent mitochondrial washing/pelleting steps. This term also refers to findings of Strange et al., who reported, by dilution studies, that a profound part of mitochondrial bound bile salts is not readily releasable, i.e., tightly bound [55].

Assuming an equal distribution in a hepatocyte volume of 3.4×10^{-9} ml [59], an estimated amount of one thousand mitochondria per hepatocyte [60] and a protein content of roughly 1 mg for 10^{10} liver mitochondria [61], an intra-hepatocyte bile salt concentration of 800 μM means an in vivo challenge of 2–3 nmol bile salts per mg of liver mitochondrial protein. In our in vitro settings, we have exposed isolated rat liver mitochondria to concentrations ranging from 125 to 500 μM bile salts, equivalent to doses of 333–1333 nmol/mg mitochondrial protein, respectively. This is, at first sight, a significantly higher challenge as the estimated 2–3 nmol/mg that would occur in vivo. However, as we have determined by gas chromatography, in our experimental in vitro setting only a very small amount (below 1%) of these bile salts bind strongly enough to mitochondria not to be immediately washed away (Table 1). And it is reasonable to assume that it is this tightly binding amount of bile salts that is responsible for the observed strong mitochondrial membrane alterations such as the displacement of the inner boundary membrane (Figs. 3, 4) or the MPT (Figs. 1–3). In

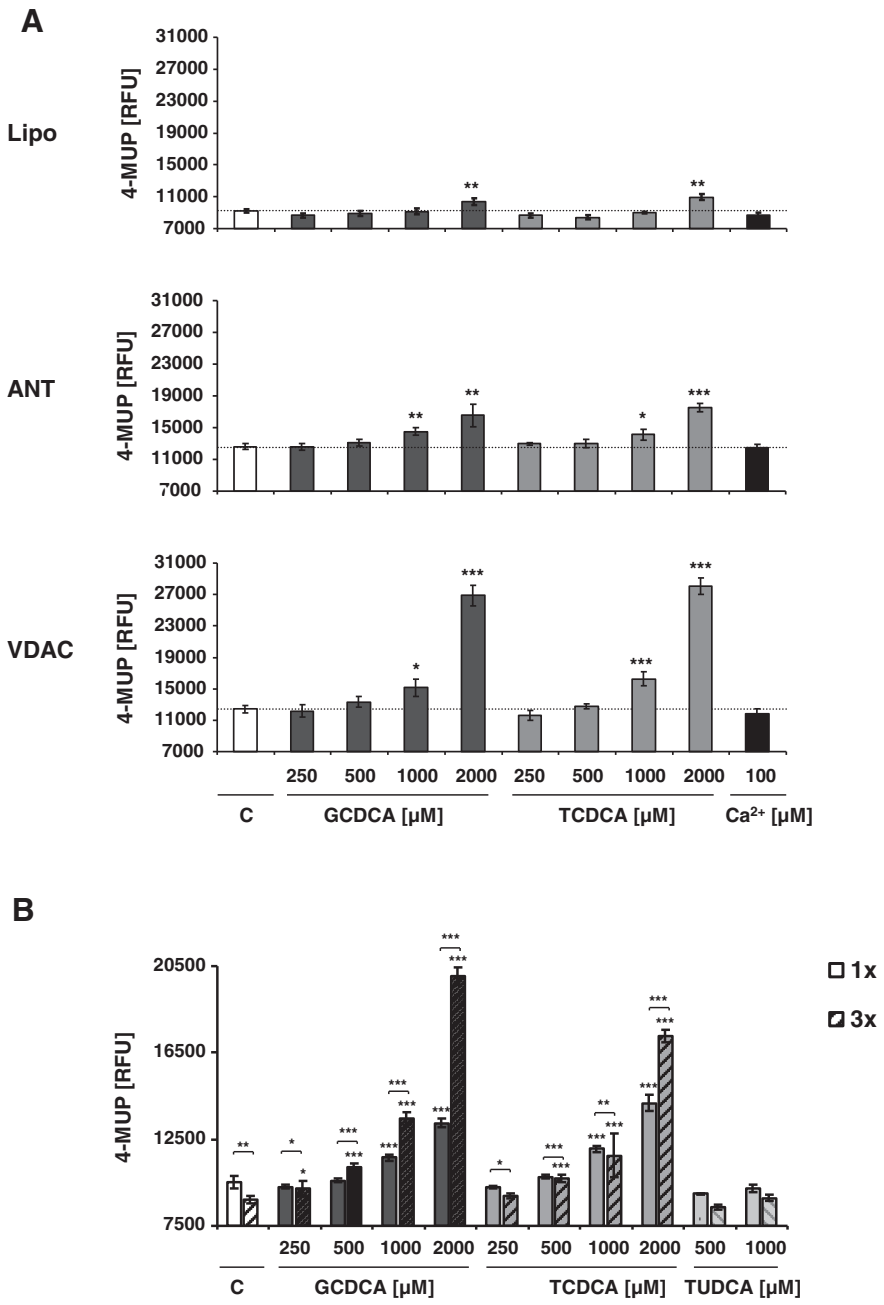

Fig. 5. Integral mitochondrial membrane proteins mediate bile salt toxicities. A Sensitivity towards bile salts of phosphatidylcholine liposomes with/without incorporated mitochondrial membrane proteins ANT or VDAC. From two independent preparations, one typical measurement with 2–4 technical replicates, each, is displayed. Maximal 4-MUP release was determined by administration of Triton X-100 (Fig. S4A). Stars depict p-values of liposomes or ANT-/VDAC-proteoliposomes against controls. B Sensitivity towards bile salts increases with the liposomal ANT content, shown in 1x vs. 3x ANT-proteoliposomes. One typical measurement out of three independent preparations with 4–5 technical replicates, each, is displayed. Maximal 4-MUP release was determined by administration of Triton X-100 (Fig. S4B). Lower stars depict p-values of 1x- and 3x-ANT-proteoliposomes against controls, upper stars are 3x- against 1x-ANT.

agreement with this assumption, we observed that TUDCA barely binds to mitochondria (Table 1) and does not induce the MPT (Fig. 1, 3B). Thus, with respect to the tightly binding bile salts, TCDCA binding efficiency was the highest with 0.89% (Table 1). Taking some further bile salt losses due to outer membrane removal into account, we therefore estimate that, in our experimental setting, roughly 1% of the exposed bile salts bind tightly enough to elicit a subsequent mitochondrial impairment. This would correspond to an in vitro challenge of 3.3–13.3 nmol tightly binding bile salts per mg mitochondrial protein, and is only slightly higher but in the order of magnitude of the above estimated values for the in vivo conditions. In fact, exposing susceptible hepatocytes to bile salts result within hours in mitochondrial structure alterations, MMP loss and cell death initiation (unpublished observations and Ref. [43]) highly similar to those findings with isolated mitochondria. Thus, the chosen conditions in our study correlate with the conditions observed in pathological cholestasis situations in hepatocytes.

5.2. The sequence of mitochondrial destruction by bile salts

How do bile salts change the mitochondrial membrane structure culminating in elicit of the MPT? Using ZE-FFE deflection, electron micrographs and immuno-blotting, we noticed that the more the mitochondria lose their outer membrane, the less amounts of bile salts can be detected in their remnant structures (Fig. 3 and Table 1).

Therefore, the outer mitochondrial membrane appears to be the crucial and major target for bile salts. Here, the structural similarities of bile salts to another steroid-bearing detergent, digitonin, are intriguing. It has been known for a long time that digitonin is able to selectively dismantle the outer mitochondrial membrane which results in intact inner membrane vesicles (IMVs) [62,63]. Thus, both steroid-bearing detergents, bile salts and digitonin, attack the mitochondrial outer membrane. Moreover, mitochondria treated by digitonin also show "finger-like extensions" of the inner membrane [63,64], similar to the inner membrane structures that we observed upon TCDCA challenge (Fig. 4III, IV and VI). As suggested by Hackenbrock and Miller [64], such extensions form when the outer and inner mitochondrial membranes largely detach but still have residual contacts between them. Indeed, the sequence of the inner mitochondrial membrane changes starting from controls to 10 min TCDCA treatment are congruent with this scenario (Fig. 4II → IV → VI). It thus appears that the tight binding of the bile salts to the outer membrane together with their detergent properties causes a massive detachment of the outer and inner (boundary) membranes (Fig. 4IV and VI).

How do bile salts cause the removal of the outer membrane? In clear contrast to the above discussed similarities to the digitonin induced structure alterations, TCDCA treated mitochondria still possess a largely intact outer membrane at the early time points (Fig. 4IV and VI). Upon digitonin exposure, however, the outer membrane is immediately removed and only small leftovers remain at the distal ends of the inner membrane extensions [64]. We did not observe such residual outer membrane vesicles in bile salt treated mitochondria (Figs. 3, 4 and S3). Rather the IMVs resulting from bile salt exposure present the picture of a full blown MOMP, highly similar to the IMVs resulting from the calcium induced MPT (Figs. 3, 4 and S3). Moreover, the occurrence of these IMVs is paralleled by an MMP-loss (Fig. 2D), a clear indication of the MPT [1,5]. On the contrary, the digitonin treated mitochondria of the above studies did not show inner membrane impairments and even their coupling between MMP and oxidative phosphorylation remained to some extent intact [63]. Therefore, although bile salts tightly bind to the outer membrane and provoke a detachment of the inner boundary membrane and cristae alterations, they do not simply dissolve the outer membrane like digitonin does, but they do induce the MPT. This, however, means that the bile salts cannot exclusively locate to the outer membrane, as they have to attack the inner membrane, since the MPT is primarily an inner membrane event [5]. In line with this prediction, a small but detectable amount of bile salts was still present in IMVs resulting upon bile salt exposure (Table 1). For example, upon a 500 μM GCDCA treatment, the resulting IMVs do not possess a residual outer membrane (Fig. 3D, 3F) but a remainder of tightly bound bile salts (Table 1). It therefore appears that, under the chosen bile salt concentrations, it is the MPT which causes the outer membrane removal via MOMP and not a dissolving detergent/digitonin-like effect on the outer membrane.

5.3. The mitochondrial target structures of bile salts

What are the targets for bile salts to induce MPT? Bile salts initially detach the inner boundary membrane from the outer membrane (Figs. 3, 4). However, many punctuate contacts between the outer and the inner membranes remain (Figs. 3E-III, 4III, VI). As the major part of bile salts locates to the outer membrane and only small parts to the inner membrane (Table 1), it is at these remaining contacts where the inner membrane is most closely confronted with the high bile salt amounts in the outer membrane. Thus, it is likely that the inner membrane is permeabilized in these regions. Although there is a continuous debate about the molecular composition of such contacts between mitochondrial outer and inner membranes, there is good agreement that they are specifically enriched in VDAC and ANT [65–68]. We have therefore tested the specific sensitivity of ANT and VDAC towards bile salts. Both proteins were purified and incorporated into dye-loaded liposomes of identical phospholipid composition (Figs. 5A, S4A). While, at this point, this approach neglects the specific presence of cholesterol and cardiolipin in the mitochondrial outer and inner membranes, respectively, we have chosen this identical phospholipid composition for the reconstituted proteoliposomes in order to focus the experimental differences here on the embedded membrane proteins (see also below). As detected by a significantly higher dye release, a pronounced membrane permeabilization occurred upon bile salt challenges in these proteoliposomes in comparison to phosphatidylcholine-liposomes (Fig. 5A). Thus, membrane proteins are the likely mediators of the bile salt elicited MPT. Both ANT- and VDAC-proteoliposomes released similar dye amounts, but the total dye load of the VDAC-proteoliposomes almost doubled the 4-MUP content of ANT-proteoliposomes (Fig. S4A). These results suggest that ANT-proteoliposomes are more sensitive towards bile salts compared to VDAC-proteoliposomes. Moreover, in ANT-proteoliposomes, a slight dye release can already be detected at 250 μM TCDCA or 500 μM GCDCA, and becomes highly significant at 1000 μM (Fig. 5A, ANT). TUDCA, which has no effect on mitochondria, is also without effect on ANT-proteoliposomes (Fig. 5B). Finally, upon a threefold enrichment of the liposomal ANT-content these proteoliposomes were even more sensitive towards GCDCA and TCDCA if directly compared to proteoliposomes with lower ANT content (Fig. 5B). Therefore ANT is one crucial executor for bile salt derived destruction.

As mentioned, these results were obtained from proteoliposomes, neither with implemented cholesterol, which is mainly present in the outer membrane, nor cardiolipin, an inner membrane lipid class. Interestingly, in first attempts to mimic the outer membrane lipid composition more closely (i.e. by implementation of cholesterol), we have found, upon bile salt challenges, tendencies towards a destabilization on VDAC-proteoliposomes and a stabilization of ANT-proteoliposomes, respectively (data not shown). Moreover, Lieser et al. [69] have reported an increase in the mitochondrial cardiolipin content as a protective/adaptive mechanism to resist cell death elicit in cholestasis. Taken together, these data clearly indicate that the respective lipids affect the bile salt provoked vulnerability of the mitochondrial membranes. However, such modified mitochondria or proteoliposomes still undergo a bile salt induced membrane permeabilization, although with altered kinetics. It therefore appears plausible that cholesterol and cardiolipin may modify the mitochondrial membrane vulnerability towards bile salts, not contradictory to the herein reported ANT as major target for bile salts. As ANT is a highly abundant inner membrane protein, it may present the "tip of the iceberg" of further bile salt targets in mitochondria.

A further issue to consider from our results in future research is the question how the bile salts pass from the outer to the inner mitochondrial membrane to execute MPT induction. On the one hand, mitochondrial bound bile salt may migrate within the membrane, potentially using mitochondrial contact sites as entrance to the inner membrane. On the other hand, bile salts may "hi-jack" mitochondrial transfer processes and/or carriers for steroids to direct bile salts to the inner membrane. A tempting yet speculative candidate is the mitochondrial benzodiazepine receptor (TSPO). TSPO locates preferentially at the mitochondrial contact site and physiologically delivers cholesterol from the cytosol to the inner membrane (Ref. [70] and references therein). Thereto TSPO possesses a cholesterol recognition amino acid consensus (CRAC) domain in its cytosol-located C-terminus [71,72], which may be accessible for bile salts as well. Moreover, in silico, we determined such potential CRAC motives in rat ANT (isoform 2, amino acids 128–138, 161–171, 226–235 and 287–296), which would mainly reside in the ANT inner transmembrane parts [73]. It will be interesting to see whether this route is employed by bile salts to attack the inner membrane.

Finally, how do bile salts exert their deleterious action on mitochondrial membranes? As discussed above, bile salts tightly bind to biological membranes and due to interacting forces with lipids or proteins their orientation may change (recently reviewed in Refs. [57,58]). This

behavior will inevitably interfere with the microenvironments of the mitochondrial membranes. In fact, recent atomic force microscopy (AFM) imaging studies have shown that the addition of bile salts to phospholipid monolayers disrupts their phase behavior and effectively "solubilises" liquid condensed domains into liquid expanded regions [57,74]. AFM has further demonstrated the capability of bile salts to displace proteins from oil–water interfaces or collapse protein networks [57,75]. Especially an integrity loss of the highly organized protein network of the mitochondrial inner membrane, exemplified by our results on ANT-proteoliposomes, may inevitably lead to MPT. These findings and considerations strongly point out at the "alternative" mechanistic model for the bile salt evoked MPT [12]. This model suggests that the inner membrane is permeabilized by misfoldings/deteriorations of native membrane proteins which forces aqueous channels to be built.

6. Conclusion

We find that the extent of bile salt induced mitochondrial impairment is bile salt species-, dose- and time-dependent. Especially at early time points of exposure we observed only a partial Cyt C loss (Fig. 4 VI), but an intact MMP (Fig. 2D), whereas at later time points or at high bile salt concentrations MMP-loss and MPT massively destroy mitochondria. This sequential mitochondrial destruction provides a strong explanation for the clinically observed switch from apoptosis to necrosis in consequence to elevated doses of bile salts [23,76,77]. It suggests that hepatocytes that have to face short-term or low-dose bile salt burdens may undergo apoptosis due to a limited mitochondrial impairment. On the contrary, a long-term or massive bile salt stress, especially in the presence of elevated calcium levels, causes irreversible mitochondrial destructions which may lead to necrosis. It is noteworthy that cell-toxic bile salts do also elicit the MPT, although delayed, when their MMP has been destroyed by FCCP (Figs. 1, S2E, F, S3D). This suggests that severe mitochondrial damages can occur at later stages, well beyond the acute phase of cholestasis and it implies that measures against this mitochondrial destruction should intervene at the earliest possible step. From a pharmacological perspective, it is the binding of bile salts to mitochondria that needs to be avoided.

Acknowledgements

The authors declare that no conflict of interest exists and would like to thank Drs. E.E. Rojo, S. Hohenester and S. Müller for their very helpful discussions and D. Wartini and B. Ledermann for their excellent technical support. This study was supported by the Deutsche Forschungsgemeinschaft (DFG) grant RU742/6-1 to CR and HZ.

Author contributions: Conceived and designed the experiments: SSchu, SSchm, DK, CBJ, CR, HZ. Performed the experiments: SSchu, SSchm, RW, MA, JL, CE, RA. Analyzed the data: SSchu, SSchm, RW, SE, FT, AW, DK, CBJ, CR, HZ. Wrote the paper: SSchu, CR, HZ.

Appendix A. Supplementary data

Supplementary data to this article can be found online at http://dx.doi.org/10.1016/j.bbamem.2013.05.007.

References

[1] D.R. Hunter, R.A. Haworth, J.H. Southard, Relationship between configuration, function, and permeability in calcium-treated mitochondria, J. Biol. Chem. 251 (1976) 5069–5077.
[2] V. Petronilli, C. Cola, P. Bernardi, Modulation of the mitochondrial cyclosporin A-sensitive permeability transition pore. II. The minimal requirements for pore induction underscore a key role for transmembrane electrical potential, matrix pH, and matrix Ca2+, J. Biol. Chem. 268 (1993) 1011–1016.
[3] M.G. Vander Heiden, N.S. Chandel, E.K. Williamson, P.T. Schumacker, C.B. Thompson, Bcl-xL regulates the membrane potential and volume homeostasis of mitochondria, Cell 91 (1997) 627–637.
[4] C. Brenner, S. Grimm, The permeability transition pore complex in cancer cell death, Oncogene 25 (2006) 4744–4756.
[5] P. Bernardi, A. Krauskopf, E. Basso, V. Petronilli, E. Blachly-Dyson, F. Di Lisa, M.A. Forte, The mitochondrial permeability transition from in vitro artifact to disease target, FEBS J. 273 (2006) 2077–2099.
[6] S. Grimm, D. Brdiczka, The permeability transition pore in cell death, Apoptosis 12 (2007) 841–855.
[7] G. Kroemer, L. Galluzzi, C. Brenner, Mitochondrial membrane permeabilization in cell death, Physiol. Rev. 87 (2007) 99–163.
[8] M. Crompton, S. Virji, J.M. Ward, Cyclophilin-D binds strongly to complexes of the voltage-dependent anion channel and the adenine nucleotide translocase to form the permeability transition pore, Eur. J. Biochem. 258 (1998) 729–735.
[9] A.P. Halestrap, A pore way to die: the role of mitochondria in reperfusion injury and cardioprotection, Biochem. Soc. Trans. 38 (2010) 841–860.
[10] N.E. Saris, E. Carafoli, A historical review of cellular calcium handling, with emphasis on mitochondria, Biochemistry (Mosc.) 70 (2005) 187–194.
[11] C.P. Baines, R.A. Kaiser, T. Sheiko, W.J. Craigen, J.D. Molkentin, Voltage-dependent anion channels are dispensable for mitochondrial-dependent cell death, Nat. Cell Biol. 9 (2007) 550–555.
[12] L. He, J.J. Lemasters, Regulated and unregulated mitochondrial permeability transition pores: a new paradigm of pore structure and function? FEBS Lett. 512 (2002) 1–7.
[13] A.P. Halestrap, Calcium, mitochondria and reperfusion injury: a pore way to die, Biochem. Soc. Trans. 34 (2006) 232–237.
[14] K.W. Kinnally, B. Antonsson, A tale of two mitochondrial channels, MAC and PTP, in apoptosis, Apoptosis (2007).
[15] Y. Tsujimoto, S. Shimizu, Role of the mitochondrial membrane permeability transition in cell death, Apoptosis 12 (2007) 835–840.
[16] D.R. Green, G. Kroemer, The pathophysiology of mitochondrial cell death, Science 305 (2004) 626–629.
[17] M.V. Berridge, P.M. Herst, A. Lawen, Targeting mitochondrial permeability in cancer drug development, Mol. Nutr. Food Res. 53 (2009) 76–86.
[18] C. Rust, N. Wild, C. Bernt, T. Vennegeerts, R. Wimmer, U. Beuers, Bile acid-induced apoptosis in hepatocytes is caspase-6-dependent, J. Biol. Chem. 284 (2009) 2908–2916.
[19] K. Dilger, S. Hohenester, U. Winkler-Budenhofer, B.A. Bastiaansen, F.G. Schaap, C. Rust, U. Beuers, Effect of ursodeoxycholic acid on bile acid profiles and intestinal detoxification machinery in primary biliary cirrhosis and health, J. Hepatol. 57 (2012) 133–140.
[20] C. Rust, K. Bauchmuller, P. Fickert, A. Fuchsbichler, U. Beuers, Phosphatidylinositol 3-kinase-dependent signaling modulates taurochenodeoxycholic acid-induced liver injury and cholestasis in perfused rat livers, Am. J. Physiol. Gastrointest. Liver Physiol. 289 (2005) G88–94.
[21] M.J. Perez, O. Briz, Bile-acid-induced cell injury and protection, World J. Gastroenterol. 15 (2009) 1677–1689.
[22] S. Hohenester, A. Gates, R. Wimmer, U. Beuers, M.S. Anwer, C. Rust, C.R. Webster, Phosphatidylinositol-3-kinase p110gamma contributes to bile salt-induced apoptosis in primary rat hepatocytes and human hepatoma cells, J. Hepatol. 53 (2010) 918–926.
[23] C.M. Palmeira, A.P. Rolo, Mitochondrially-mediated toxicity of bile acids, Toxicology 203 (2004) 1–15.
[24] A.P. Rolo, P.J. Oliveira, A.J. Moreno, C.M. Palmeira, Bile acids affect liver mitochondrial bioenergetics: possible relevance for cholestasis therapy, Toxicol. Sci. 57 (2000) 177–185.
[25] R. Botla, J.R. Spivey, H. Aguilar, S.F. Bronk, G.J. Gores, Ursodeoxycholate (UDCA) inhibits the mitochondrial membrane permeability transition induced by glycochenodeoxycholate: a mechanism of UDCA cytoprotection, J. Pharmacol. Exp. Ther. 272 (1995) 930–938.
[26] G.J. Gores, H. Miyoshi, R. Botla, H.I. Aguilar, S.F. Bronk, Induction of the mitochondrial permeability transition as a mechanism of liver injury during cholestasis: a potential role for mitochondrial proteases, Biochim. Biophys. Acta 1366 (1998) 167–175.
[27] H. Zischka, N. Larochette, F. Hoffmann, D. Hamoller, N. Jagemann, J. Lichtmannegger, L. Jennen, J. Muller-Hocker, F. Roggel, M. Gottlicher, A.M. Vollmar, G. Kroemer, Electrophoretic analysis of the mitochondrial outer membrane rupture induced by permeability transition, Anal. Chem. 80 (2008) 5051–5058.
[28] H.G. Heidrich, R. Stahn, K. Hannig, The surface charge of rat liver mitochondria and their membranes, Clarification of some controversies concerning mitochondrial structure, J Cell Biol 46 (1970) 137–150.
[29] P.X. Petit, M. Goubern, P. Diolez, S.A. Susin, N. Zamzami, G. Kroemer, Disruption of the outer mitochondrial membrane as a result of large amplitude swelling: the impact of irreversible permeability transition, FEBS Lett. 426 (1998) 111–116.
[30] N. Zamzami, D. Metivier, G. Kroemer, Quantitation of mitochondrial transmembrane potential in cells and in isolated mitochondria, Methods Enzymol. 322 (2000) 208–213.
[31] H. Zischka, J. Lichtmannegger, N. Jagemann, L. Jennen, D. Hamoller, E. Huber, A. Walch, K.H. Summer, M. Gottlicher, Isolation of highly pure rat liver mitochondria with the aid of zone-electrophoresis in a free flow device (ZE-FFE), Methods Mol. Biol. 424 (2008) 333–348.
[32] H. Eubel, C.P. Lee, J. Kuo, E.H. Meyer, N.L. Taylor, A.H. Millar, Free-flow electrophoresis for purification of plant mitochondria by surface charge, Plant J. 52 (2007) 583–594.
[33] S. Hartwig, C. Feckler, S. Lehr, K. Wallbrecht, H. Wolgast, D. Muller-Wieland, J. Kotzka, A critical comparison between two classical and a kit-based method for mitochondria isolation, Proteomics 9 (2009) 3209–3214.
[34] H. Zischka, N. Kinkl, R.J. Braun, M. Ueffing, Purification of *Saccharomyces cerevisiae* mitochondria by zone electrophoresis in a free flow device, Methods Mol. Biol. 432 (2008) 51–64.

[35] K.M. Fuller, E.A. Arriaga, Capillary electrophoresis monitors changes in the electrophoretic behavior of mitochondrial preparations, J. Chromatogr. B Analyt. Technol. Biomed. Life Sci. 806 (2004) 151–159.
[36] H. Zischka, R.J. Braun, E.P. Marantidis, D. Buringer, C. Bornhovd, S.M. Hauck, O. Demmer, C.J. Gloeckner, A.S. Reichert, F. Madeo, M. Ueffing, Differential analysis of *Saccharomyces cerevisiae* mitochondria by free flow electrophoresis, Mol. Cell. Proteomics 5 (2006) 2185–2200.
[37] A. Ruck, M. Dolder, T. Wallimann, D. Brdiczka, Reconstituted adenine nucleotide translocase forms a channel for small molecules comparable to the mitochondrial permeability transition pore, FEBS Lett. 426 (1998) 97–101.
[38] V. de Pinto, G. Prezioso, F. Palmieri, A simple and rapid method for the purification of the mitochondrial porin from mammalian tissues, Biochim. Biophys. Acta 905 (1987) 499–502.
[39] A.S. Belzacq, E. Jacotot, H.L. Vieira, D. Mistro, D.J. Granville, Z. Xie, J.C. Reed, G. Kroemer, C. Brenner, Apoptosis induction by the photosensitizer verteporfin: identification of mitochondrial adenine nucleotide translocator as a critical target, Cancer Res. 61 (2001) 1260–1264.
[40] R. Hovius, H. Lambrechts, K. Nicolay, B. de Kruijff, Improved methods to isolate and subfractionate rat liver mitochondria, Lipid composition of the inner and outer membrane, Biochim Biophys Acta 1021 (1990) 217–226.
[41] G. Daum, Lipids of mitochondria, Biochim. Biophys. Acta 822 (1985) 1–42.
[42] H. Towbin, T. Staehelin, J. Gordon, Electrophoretic transfer of proteins from polyacrylamide gels to nitrocellulose sheets: procedure and some applications, Proc. Natl. Acad. Sci. U.S.A. 76 (1979) 4350–4354.
[43] G.U. Denk, C.P. Kleiss, R. Wimmer, T. Vennegeerts, F. Reiter, S. Schulz, H. Zischka, C. Rust, Tauro-beta-muricholic acid restricts bile acid-induced hepatocellular apoptosis by preserving the mitochondrial membrane potential, Biochem Biophys Res Commun (2012).
[44] L. Maillette de Buy Wenniger, U. Beuers, Bile salts and cholestasis, Dig. Liver Dis. 42 (2010) 409–418.
[45] H. Greim, P. Czygan, F. Schaffner, H. Popper, Determination of bile acids in needle biopsies of human liver, Biochem. Med. 8 (1973) 280–286.
[46] J.R. Spivey, S.F. Bronk, G.J. Gores, Glycochenodeoxycholate-induced lethal hepatocellular injury in rat hepatocytes, Role of ATP depletion and cytosolic free calcium, J Clin Invest 92 (1993) 17–24.
[47] M. Crompton, H. Ellinger, A. Costi, Inhibition by cyclosporin A of a Ca^{2+}-dependent pore in heart mitochondria activated by inorganic phosphate and oxidative stress, Biochem. J. 255 (1988) 357–360.
[48] D.G. Nicholls, S.J. Ferguson, Bioenergetics 2, Academic Press, San Diego, 1992.
[49] V. Petronilli, C. Cola, S. Massari, R. Colonna, P. Bernardi, Physiological effectors modify voltage sensing by the cyclosporin A-sensitive permeability transition pore of mitochondria, J. Biol. Chem. 268 (1993) 21939–21945.
[50] S.B. Berman, S.C. Watkins, T.G. Hastings, Quantitative biochemical and ultrastructural comparison of mitochondrial permeability transition in isolated brain and liver mitochondria: evidence for reduced sensitivity of brain mitochondria, Exp. Neurol. 164 (2000) 415–425.
[51] S. Hohenester, L.M. Wenniger, C.C. Paulusma, S.J. van Vliet, D.M. Jefferson, R.P. Elferink, U. Beuers, A biliary HCO_3^- umbrella constitutes a protective mechanism against bile acid-induced injury in human cholangiocytes, Hepatology 55 (2012) 173–183.
[52] S. Guldutuna, G. Zimmer, M. Leuschner, S. Bhatti, A. Elze, B. Deisinger, M. Hofmann, U. Leuschner, The effect of bile salts and calcium on isolated rat liver mitochondria, Biochim. Biophys. Acta 1453 (1999) 396–406.
[53] A.F. Hofmann, Bile acids: the good, the bad, and the ugly, News Physiol. Sci. 14 (1999) 24–29.
[54] T. Okishio, P.P. Nair, Studies on bile acids, Some observations on the intracellular localization of major bile acids in rat liver, Biochemistry 5 (1966) 3662–3668.
[55] R.C. Strange, B.T. Chapman, J.D. Johnston, I.A. Nimmo, I.W. Percy-Robb, Partitioning of bile acids into subcellular organelles and the in vivo distribution of bile acids in rat liver, Biochim. Biophys. Acta 573 (1979) 535–545.
[56] D.A. Fahey, M.C. Carey, J.M. Donovan, Bile acid/phosphatidylcholine interactions in mixed monomolecular layers: differences in condensation effects but not interfacial orientation between hydrophobic and hydrophilic bile acid species, Biochemistry 34 (1995) 10886–10897.
[57] J. Maldonado-Valderrama, P. Wilde, A. Macierzanka, A. Mackie, The role of bile salts in digestion, Adv. Colloid Interface Sci. 165 (2011) 36–46.
[58] D. Madenci, A. Salonen, P. Schurtenberger, J.S. Pedersen, S.U. Egelhaaf, Simple model for the growth behaviour of mixed lecithin-bile salt micelles, Phys. Chem. Chem. Phys. 13 (2011) 3171–3178.
[59] In: H. Lodish, A. Berk, S.L. Zipursky, P. Matsudaira, D. Baltimore, J.E. Darnell (Eds.), Molecular Cell Biology, 5th ed., W. H. Freeman and Company, New York, 2000.
[60] In: I.E. Scheffler (Ed.), Mitochondria, 2nd ed., John Wiley & Sons, Inc., Hoboken, New Jersey, 2008.
[61] K. Schwerzmann, L.M. Cruz-Orive, R. Eggman, A. Sanger, E.R. Weibel, Molecular architecture of the inner membrane of mitochondria from rat liver: a combined biochemical and stereological study, J. Cell Biol. 102 (1986) 97–103.
[62] C.S. Boyer, E.P. Neve, G.A. Moore, P. Moldeus, Effect of mitochondrial protein concentration on the efficiency of outer membrane removal by the cholesterol-selective detergent digitonin, Biochim. Biophys. Acta 1190 (1994) 304–308.
[63] C. Schnaitman, J.W. Greenawalt, Enzymatic properties of the inner and outer membranes of rat liver mitochondria, J. Cell Biol. 38 (1968) 158–175.
[64] C.R. Hackenbrock, K.J. Miller, The distribution of anionic sites on the surfaces of mitochondrial membranes, Visual probing with polycationic ferritin, J Cell Biol 65 (1975) 615–630.
[65] O. Speer, N. Back, T. Buerklen, D. Brdiczka, A. Koretsky, T. Wallimann, O. Eriksson, Octameric mitochondrial creatine kinase induces and stabilizes contact sites between the inner and outer membrane, Biochem. J. 385 (2005) 445–450.
[66] C. Hoppel, J. Kerner, P. Turkaly, P. Minkler, B. Tandler, Isolation of hepatic mitochondrial contact sites: previously unrecognized inner membrane components, Anal. Biochem. 302 (2002) 60–69.
[67] D.G. Brdiczka, D.B. Zorov, S.S. Sheu, Mitochondrial contact sites: their role in energy metabolism and apoptosis, Biochim. Biophys. Acta 1762 (2006) 148–163.
[68] A.S. Reichert, W. Neupert, Contact sites between the outer and inner membrane of mitochondria-role in protein transport, Biochim. Biophys. Acta 1592 (2002) 41–49.
[69] M.J. Lieser, J. Park, S. Natori, B.A. Jones, S.F. Bronk, G.J. Gores, Cholestasis confers resistance to the rat liver mitochondrial permeability transition, Gastroenterology 115 (1998) 693–701.
[70] R. Rupprecht, V. Papadopoulos, G. Rammes, T.C. Baghai, J. Fan, N. Akula, G. Groyer, D. Adams, M. Schumacher, Translocator protein (18 kDa) (TSPO) as a therapeutic target for neurological and psychiatric disorders, Nat. Rev. Drug Discov. 9 (2010) 971–988.
[71] H. Li, Z. Yao, B. Degenhardt, G. Teper, V. Papadopoulos, Cholesterol binding at the cholesterol recognition/interaction amino acid consensus (CRAC) of the peripheral-type benzodiazepine receptor and inhibition of steroidogenesis by an HIV TAT-CRAC peptide, Proc. Natl. Acad. Sci. U.S.A. 98 (2001) 1267–1272.
[72] H. Li, V. Papadopoulos, Peripheral-type benzodiazepine receptor function in cholesterol transport, Identification of a putative cholesterol recognition/interaction amino acid sequence and consensus pattern, Endocrinology 139 (1998) 4991–4997.
[73] E. Pebay-Peyroula, C. Dahout-Gonzalez, R. Kahn, V. Trezeguet, G.J. Lauquin, G. Brandolin, Structure of mitochondrial ADP/ATP carrier in complex with carboxyatractyloside, Nature 426 (2003) 39–44.
[74] B.S. Chu, A.P. Gunning, G.T. Rich, M.J. Ridout, R.M. Faulks, M.S. Wickham, V.J. Morris, P.J. Wilde, Adsorption of bile salts and pancreatic colipase and lipase onto digalactosyldiacylglycerol and dipalmitoylphosphatidylcholine monolayers, Langmuir 26 (2010) 9782–9793.
[75] J. Maldonado-Valderrama, N.C. Woodward, A.P. Gunning, M.J. Ridout, F.A. Husband, A.R. Mackie, V.J. Morris, P.J. Wilde, Interfacial characterization of beta-lactoglobulin networks: displacement by bile salts, Langmuir 24 (2008) 6759–6767.
[76] T. Patel, S.F. Bronk, G.J. Gores, Increases of intracellular magnesium promote glycodeoxycholate-induced apoptosis in rat hepatocytes, J. Clin. Invest. 94 (1994) 2183–2192.
[77] A.P. Rolo, C.M. Palmeira, J.M. Holy, K.B. Wallace, Role of mitochondrial dysfunction in combined bile acid-induced cytotoxicity: the switch between apoptosis and necrosis, Toxicol. Sci. 79 (2004) 196–204.